

# Real-time in-situ thermal monitoring system and defect detection using deep learning applied to additive manufacturing

RHIM Safouene<sup>1,a\*</sup>, ALBAHLOUL Hala<sup>1,2,b</sup> and ROUA Christophe<sup>1,c</sup>

<sup>1</sup>Cogit Composites, 9117 Rue des Vignerons 18390 Saint-Germain-du-Puy, France

<sup>2</sup>Université Paris Cité, Learning planet institute, 8 Bis rue Charles V, 75004 Paris, France

<sup>a</sup>s.rhim@cogit-composites.com, <sup>b</sup>h.albahloul@cogit-composites.com,  
<sup>c</sup>christophe.roua@cogit-composites.com

**Keywords:** Additive Manufacturing, Thermography, Artificial Intelligence, Computer Vision, Deep-Learning, Defect Detection, Fused Filament Fabrication

**Abstract.** Fused deposition modeling, a widely employed additive manufacturing method, has witnessed a significant trend towards printing advanced materials such as PEEK and PAEK in recent years. Research studies have demonstrated the significance of process thermal dynamics in influencing the mechanical and geometric properties of printed components. This paper introduces a real-time thermal monitoring system that comprehensively tracks the thermal history of the printed component. Additionally, a deep learning model is presented, capable of detecting defects during the printing process. The integration of this monitoring system in a closed-loop mode offers the advantage of real-time adjustments, facilitating an immediate enhancement in the quality of the printed parts based on the continuously measured thermal data and the identified defects. Beyond real-time improvements, the data output from the monitoring system holds immense potential for broader applications. It can be seamlessly integrated into simulation software, providing a valuable dataset that can be leveraged to predict the physical properties and the adhesion quality of the printed parts.

## Introduction

Additive manufacturing, specifically the Fused Filament Fabrication (FFF) process, involves the conversion of 3D-designed components into tangible fabricated parts. The procedure starts with the creation of the part using 3D Computer-Aided Design (CAD) software. Subsequently, the design is transferred to a slicer, which generates the tool-path (G-Code). Finally, the machine executes the printing of the part based on the specified tool-path. The method consists of converting a solid filament into a semi-liquid substance through the application of a heated nozzle. Once the material reaches a molten state, it is deposited along a defined two-dimensional XY plane. The process advances layer by layer to construct a three-dimensional object.

Additive manufacturing has gained a lot of importance in the last years, especially for high performance materials (PEEK, PAEK,...) that are used in a lot of applications (aerospace, defence, medical, ...) as it showed the potential of fabricating multi-functional parts that are hard or sometimes impossible to be done using old technologies.

Like any other technology, achieving consistently high-quality 3D printed parts that satisfy industry requirements, whether in terms of mechanical properties or geometric aspects, poses inherent challenges. 3D printed components are susceptible to various defects, including under-extrusion, over-extrusion, spaghetti, and filament adhesion issues [1] as shown in Figure 1.



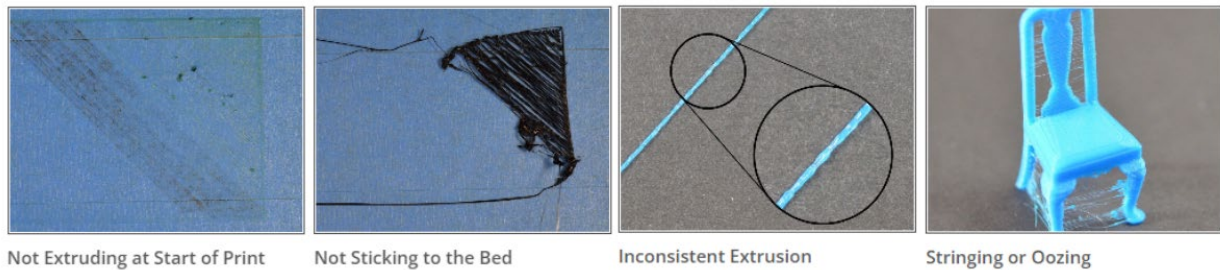


*Figure 1 : Examples of defects in 3D printed parts*

At the moment the only possible solutions to qualify printed parts often involves the implementation of post-processing quality control systems either destructive or non-destructive, that are always very expensive. Otherwise, we can opt for visual inspection alone, which is more cost-effective but lacks a quantitative assessment of the defect and cannot penetrate the core of the part. As examples of non-destructive methods, laser scanning systems that can be utilized to perform detailed dimensional inspections and identify deviations from the intended geometry, X-ray and CT scanning methods to detect internal defects and assess the structural integrity of printed parts. Destructive testing methods includes tensile, compression, fatigue...

As a consequence, considerable research has been undertaken to grasp the critical parameters impacting the quality of printed parts. Simultaneously, efforts have been directed towards identifying defects in real-time or during post-processing through the application of image processing algorithms or the utilization of deep learning models. Various configurations have been tested, employing optical or thermal cameras positioned alongside printers to achieve a comprehensive perspective of parts, demonstrating positive outcomes in terms of quality control.

Single camera approach like camera coupled with computer vision techniques [2–5] or deep learning models [3,6–8] and fixed on the side view, can detect various macro extrusion AM defects (Blobs, Under-extrusion...), but this solution have its limitation since the printer head could obscure the view which make it difficult to always view the material as it is being deposited from the nozzle.

Methods that uses algorithms for change detection or Siamese network [9] to calculate the similarity or the difference between a reference image and the real time image, can give high accurate results in addition to localize the defect. However, techniques related to similarity score, need one correct printed reference at least. This may be especially limiting for custom parts.

Techniques like multi-camera 3D structured light scanning and digital image correlation offer the potential to compare 3D reconstructions of printed parts with digital models to identify dimensional inaccuracies. It offers high accuracy measurement but it is applied either on finished parts or layer by layer so it requires pausing the printing [10,11].

Within the context of this paper, we present a comprehensive monitoring system that emphasizes the critical role of thermal measurement in the 3D printing process. Our approach extends beyond thermal monitoring by incorporating a sophisticated deep learning model, specifically trained to detect defects in real-time during the printing process. The goal of this monitoring system is to generate a digital shadow of the printed components, facilitating the inspection during the post-processing phase. Furthermore, the system can be integrated seamlessly in close-loop mode, facilitating continuous adjustments and optimizations during the printing process, thereby enhancing the overall quality and reliability of the final printed components.

This integrated approach positions our monitoring system as a robust solution for advancing the precision and quality assurance aspects of 3D printing technology.

## Experimental set-up and methods

### *Thermal monitoring solution*

Our patented thermal monitoring system [12] comprises two thermal cameras securely attached to the printing tool, enabling a complete 360° view around the nozzle as shown in the Figure 2. The captured frames from these cameras are then transmitted to a processing unit, where they are seamlessly stitched together to create a cohesive and unique output image that encapsulates the entire thermal landscape.

Additionally, the system measures and records the temperature only from the pixels located on the filament being deposited, storing this information in a file that includes a spatial point cloud of the printed part, with time-temperature evolution for each point.

The system has also the capability to measure the temperature of the area where we intend to deposit the new material which is important to ensure a good adhesion quality of the part.

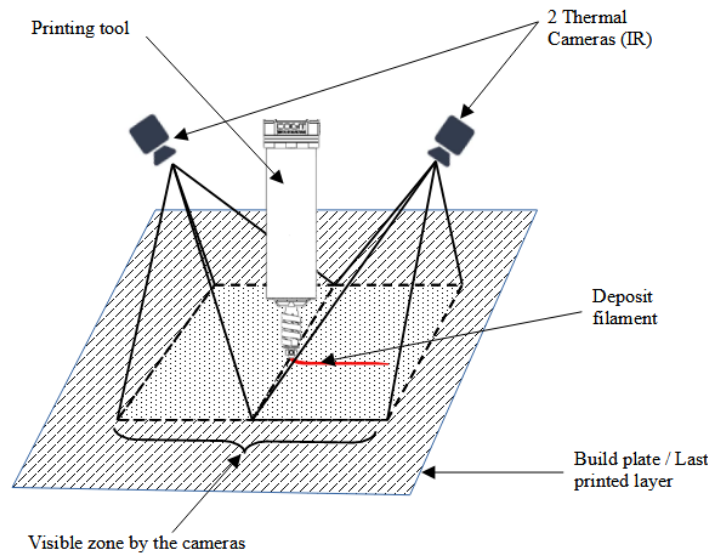


Figure 2 : Schematic representation of the thermal monitoring system

### *System configuration*

The innovative thermal monitoring system [12], engineered by COGIT COMPOSITES, is a sophisticated assembly featuring two high-performance thermal cameras. Operating seamlessly at an impressive 80 frames per second (FPS), these cameras are strategically mounted at a carefully determined angle around the printing tool. This strategic placement ensures a comprehensive coverage of thermal data throughout the printing process, these cameras generate a final stitched image with a resolution of approximately 528×370 pixels and ≈0.2 mm resolution in the printing plane.

The camera resolution is adapted to the filament width. In this study, the printed filaments measure 0.7 mm in width, allowing for at least 3 pixels per filament. This resolution is necessary to ensure the selection of the pixel at the centre of the filament. In the case of smaller filaments, a higher camera resolution is required. Similarly, for the printing of wider filaments, such resolution is not necessary.

To ensure the proper functioning of the thermal monitoring system, a series of calibration steps must be undertaken, encompassing the estimation of internal camera parameters (distortion coefficients and focal length...).

A Hand-Eye calibration also is performed to estimate the transformation between the cameras and the machine reference. To streamline this calibration process, a sophisticated procedure has

been designed to serve the specific requirements of the system and overcoming the constraint of the Cartesian machine, also a specific calibration object was adapted for thermal vision.

To initiate the monitoring system, it is necessary to previously transmit the G-code of the part needs to be printed to the processing unit. In addition to the two thermal cameras, the real-time position of the tool must be provided to the system. Whenever the printing starts, the system starts scanning the thermal evolution of the filament being deposited and generating the 5D data, as illustrated in the diagram below Figure 3.

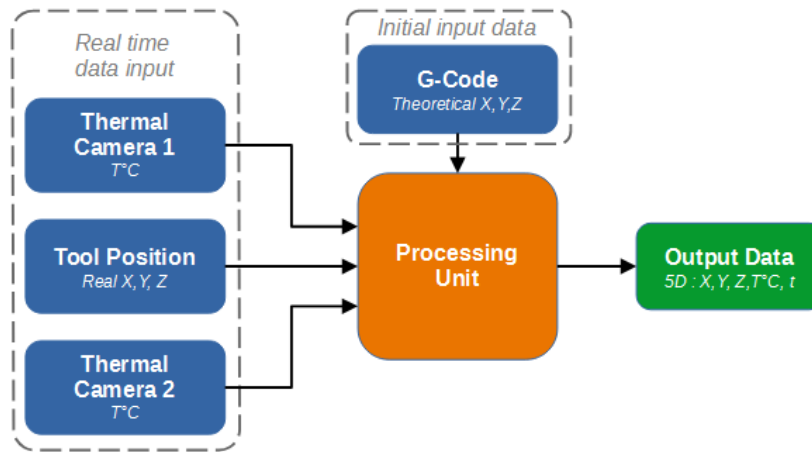


Figure 3 : Thermal monitoring system functional diagram

#### Data output

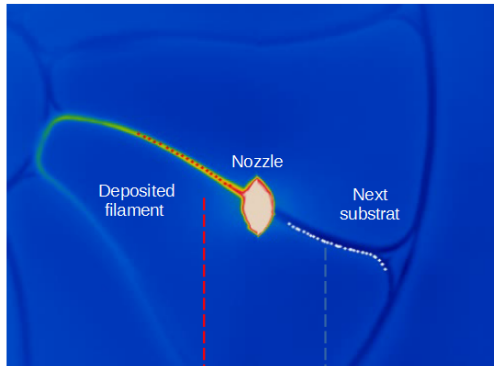
As previously described, the system is capable of monitoring the real-time temperature before and after filament deposition, as showed in Figure 4.a. The red dots represent pixels measured following filament deposition, while the white dots represent pixels measured for the subsequent filament deposition. Those measured points are then represented in the Figure 4.b in another shape for easy understanding where the temperature is function of the distance from the extruder. In this new representation, the red curve corresponds to the red dots and the blue curve corresponds to the white dots.

Additionally, all collected data is systematically recorded in an HDF5 file, organized into various datasets.

- Dataset “Time”: It’s a 1D array of values corresponding to every instant  $t$  of the collected data.
- Dataset “Position and Temperature”: It’s a 2D array, every row contains a list of  $[X, Y, Z, T^{\circ}C]$  points measured at the instant  $t$ .
- Dataset “Real Time Position”: It’s a 1D array of tool positions, every row contain the position collected at the instant  $t$ .
- Dataset “Dataset Length”: It’s a 1D array of values, every row indicates the number of points that has been measured at the instant  $t$  (Note: this dataset is added for convenience because there are empty cells in the dataset “Position and Temperature”, due to variance in the number of points measured at every instant  $t$ ).

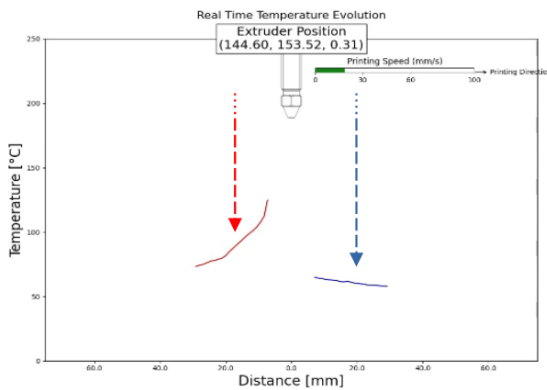
The Figure 4.c provides a clear representation of the file structure.

Step 1 : Thermal images capturing and stitching



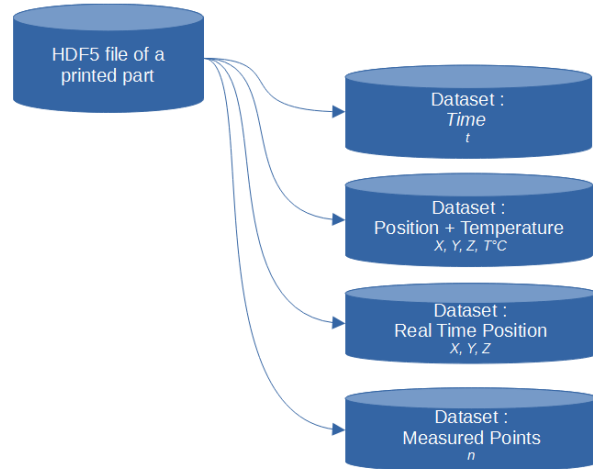
(a)

Step 2 : Points of interest measurement



(b)

Step 3 : Storing 5D data in HDF5 file



(c)

Figure 4 : Thermal measurement, points after deposition (red dots) and before deposition (white dots) (a). Temperature representation of the measured points in function of the distance to extruder (b). Stored HDF5 file structure (c)

For the purpose of visually exploring the thermal history at different time, a dedicated script has been developed to replay the content stored within the generated HDF5 file. This representation allows obtaining a digital shadow that can be used to detect defects or validate the thermal history of the parts. The provided Figure 5 serves as an example of the output digital shadow that is presented at an instant t.

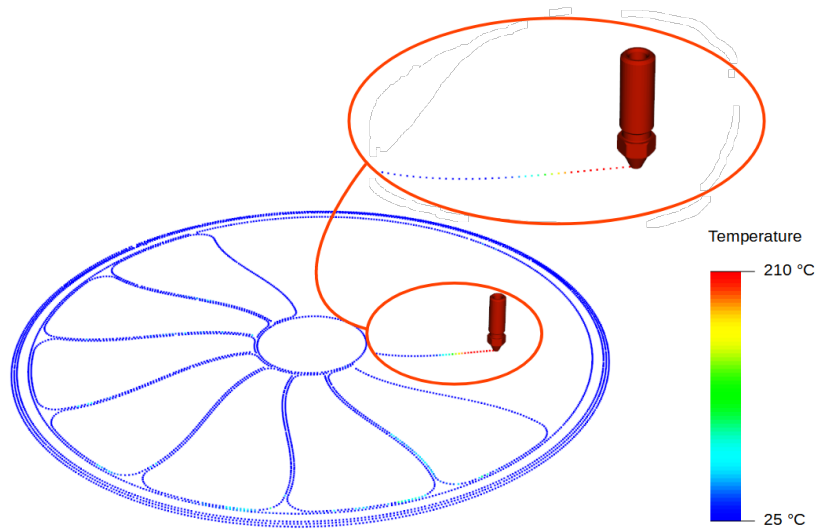


Figure 5 : Sample representation of digital shadow

### *Defect detection*

As mentioned before, the capability of the monitoring system is expanded through the development of a deep learning model with the ability to detect defects in real-time. It is assumed that distinguishable features in thermal images captured during 3D printing can be utilized to identify various types of defects. This assumption is based on the understanding that patterns associated with each defect in thermal imaging may be recognized due to heat distribution, speed, flow rate, and movement during the printing process.

As a result, an object detection model can achieve real-time and accurate detection and localization of defects, enabling the implementation of subsequent correction system.

### *Data collection – Training*

The dataset comprises thermal images captured from videos recorded during the printing process. To introduce defects, intentional modifications to printing parameters were made, either in real-time or by generating a modified G-Code using a python script.

Subsequently, these videos have been processed, and images were extracted at a rate of 10 frames per second to reduce redundancy. Before training, data augmentation techniques were applied to enhance the dataset. Existing methods from Albumentations [13] have been employed and two additional techniques have been developed: Custom Mosaic and Custom Cut Mix as shown in Figure 6.

Custom Mosaic involves generating an image by combining four distinct parts from different random images, each containing defects. This approach allows the reduction of batch size effectively.

In the context of Custom Cut Mix, the scenario presented a challenge with the original Cut Mix augmentation technique, given that the majority of objects were centred in each image, occupying various areas and sizes. The risk of cutting an empty portion from one image and pasting it onto an object, potentially obscuring it, was high. The implemented variation ensures that when cutting a random object from one image and pasting it onto another, the intersection between objects does not exceed 0.75, thereby preserving the integrity of the original object.



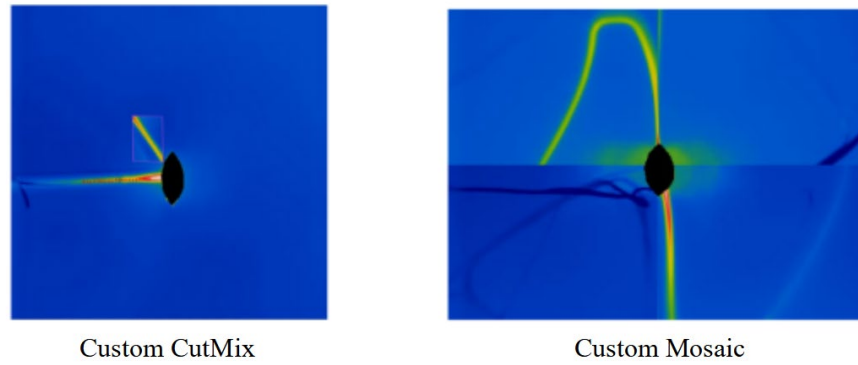


Figure 6 : Output of modified Cut Mix and Mosaic methods

The images have been categorized into seven distinct classes (No printing, Non-stick filament, Stringing, Gaps, Inconsistent extrusion, Blobs, and Hot spot). Examples of each defect in thermal images can be found in Figure 7.a (The different classes have been chosen after doing tests and analyses on the thermal images in order to avoid model confusion) and the total number of images per class is presented in Figure 7.b.

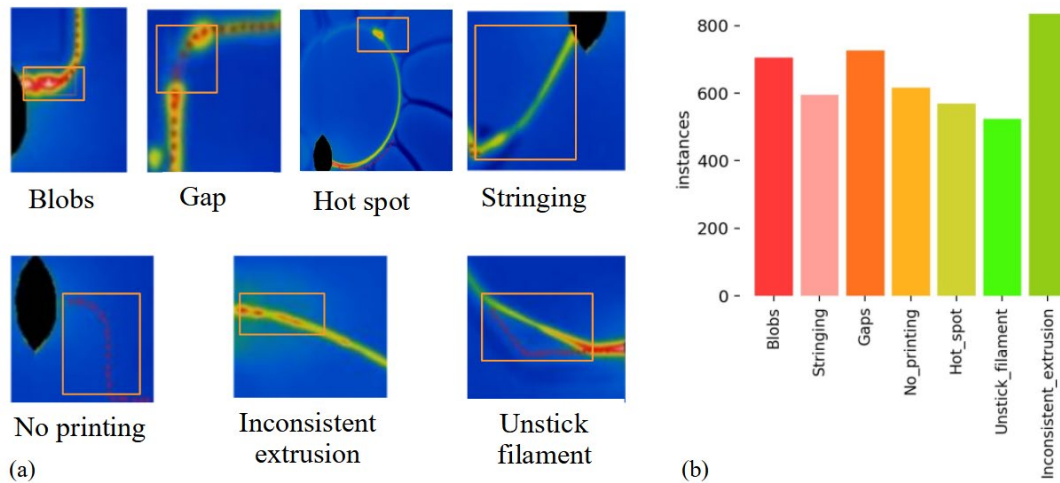


Figure 7 : Example of defects in thermal images (a), Number of images per class used for training (b)

For training, an NVIDIA RTX A2000 GPU was used. A subset of 10% of the images (images with no defects) were retained to reduce the False Positives (FP), then dataset was divided into 70% for training, 20% for validation and 10% for testing.

### Validation

Following extensive testing, the model hyper parameters have been fine-tuned and optimal features for annotation have been identified.

The ultimate model configuration yields a mAP50 of 0.91 and mAP50-95 of 0.72, as showed in the Figure 8. Additionally, the model achieved an inference speed of 5.1 ms per image on the validation dataset.

The confusion matrix shown in Figure 9 indicates favourable results across all classes, with only a slight confusion observed between hot spots and blobs. This confusion is expected, given the similar appearance of these defects in thermal images.

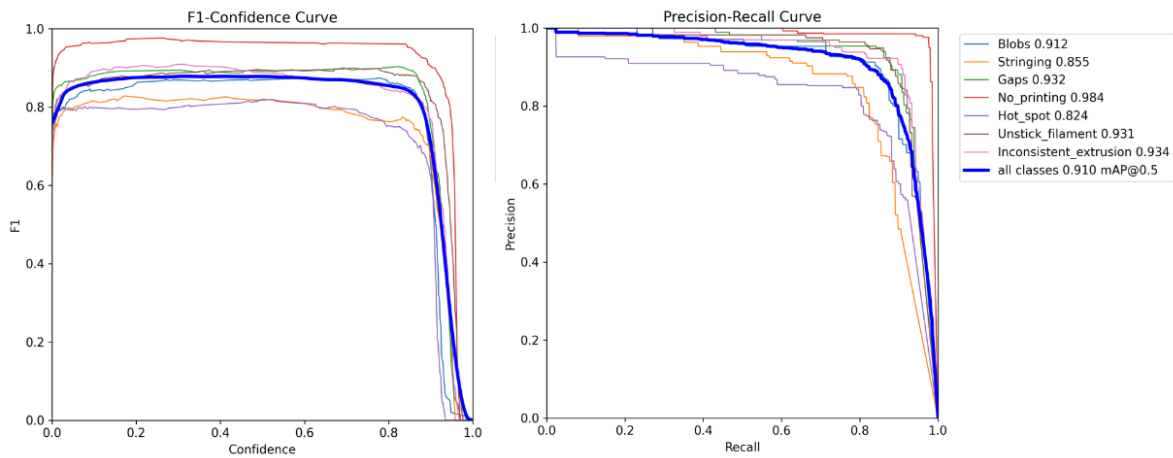


Figure 8 : Model evaluation curves

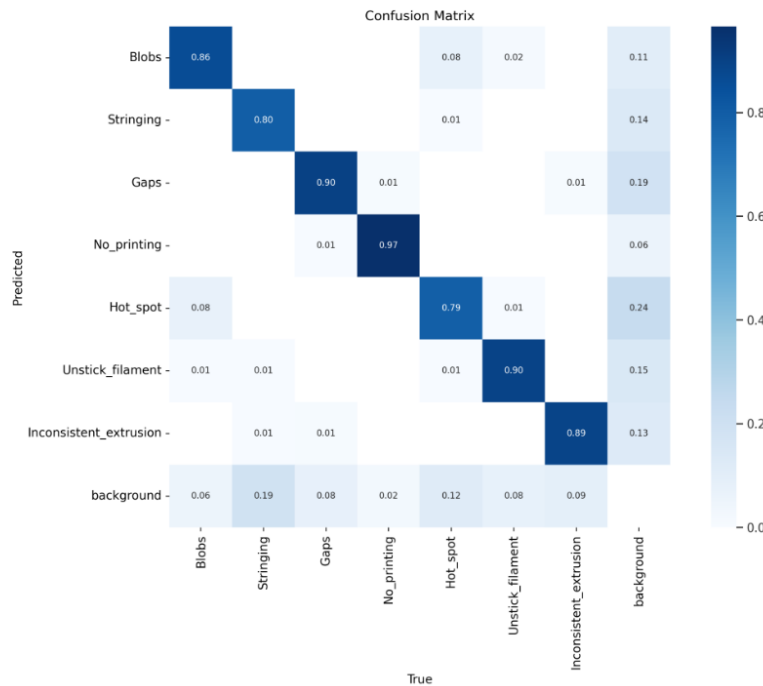


Figure 9 : Model confusion matrix

**Results and discussion**

Despite the small number of images used for training, the final model successfully identified over 90% of the defects on test videos as shown in Figure 10. Also the usage of the mosaic method resulted in a notable reduction in the required number of epochs, halving the training time while maintaining high accuracy. Furthermore, the use of MixUp augmentation with rotation and flipping increased the mAP50 by 3.2% while increased the mAP50-95 by 1.7%.

Although thermal imaging has proven effective in detecting seven types of defects, there are still some cases where certain defects remain undetected. This highlights the importance of incorporating additional information, such as speed, flow rate, temperature evolution over time of the printed filament... One approach to address this is using multi-modal learning.

An alternative approach is to combine optical imaging and thermal imaging, expanding the range of accessible features. This fusion not only increases detection precision but also facilitates the identification of additional defects.



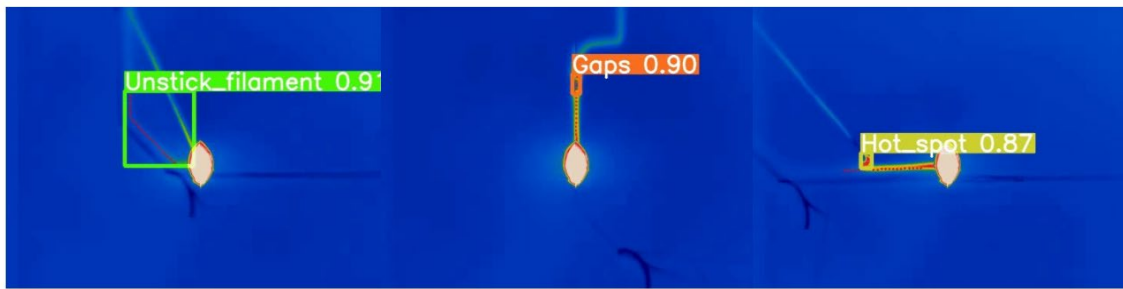


Figure 10 : Examples of detected defects using the final model

## Conclusions

In conclusion, we showed an in-situ thermal monitoring system capable of supervising the thermal evolution of the printed filament that also generates a digital shadow of the printed part.

Additionally, a deep learning model trained to detect defects achieved high accuracy in detecting and localizing 7 types of defects. Future work for improving the system involves detecting other types of defects by adding additional information for multi-modal learning and also using the system in close loop-mode in order to apply correction to the printing.

## References

- [1] Print Quality Guide n.d. <https://www.simplify3d.com/resources/print-quality-troubleshooting/>
- [2] Baumann F, Roller D. Vision based error detection for 3D printing processes. MATEC Web Conf 2016;59:06003. <https://doi.org/10.1051/mateconf/20165906003>
- [3] Brion DAJ, Pattinson SW. Generalisable 3D printing error detection and correction via multi-head neural networks. Nat Commun 2022;13:4654. <https://doi.org/10.1038/s41467-022-31985-y>
- [4] Tian X, Li Y, Ma D, Han J, Xia L. Strand width uniformly control for silicone extrusion additive manufacturing based on image processing. Int J Adv Manuf Technol 2022;119:3077–90. <https://doi.org/10.1007/s00170-021-08370-y>
- [5] Huang T, Wang S, Yang S, Dai W. Statistical process monitoring in a specified period for the image data of fused deposition modeling parts with consistent layers. J Intell Manuf 2021;32:2181–96. <https://doi.org/10.1007/s10845-020-01628-4>
- [6] Jin Z, Zhang Z, Gu GX. Automated Real-Time Detection and Prediction of Interlayer Imperfections in Additive Manufacturing Processes Using Artificial Intelligence. Adv Intell Syst 2020;2:1900130. <https://doi.org/10.1002/aisy.201900130>
- [7] Zhang Z, Fidan I, Allen M. Detection of Material Extrusion In-Process Failures via Deep Learning. Inventions 2020;5:25. <https://doi.org/10.3390/inventions5030025>
- [8] Jin Z, Zhang Z, Gu GX. Autonomous in-situ correction of fused deposition modeling printers using computer vision and deep learning. Manuf Lett 2019;22:11–5. <https://doi.org/10.1016/j.mfglet.2019.09.005>
- [9] Niu Y, Chadwick E, Ma AWK, Yang Q. Semi-Siamese Network for Robust Change Detection Across Different Domains with Applications to 3D Printing 2022. <https://doi.org/10.48550/arXiv.2212.08583>
- [10] Charalampous P, Kostavelis I, Kopsacheilis C, Tzovaras D. Vision-based real-time monitoring of extrusion additive manufacturing processes for automatic manufacturing error detection. Int J Adv Manuf Technol 2021;115:3859–72. <https://doi.org/10.1007/s00170-021-07419-2>

- [11] Holzmond O, Li X. In situ real time defect detection of 3D printed parts. *Addit Manuf* 2017;17:135–42. <https://doi.org/10.1016/j.addma.2017.08.003>
- [12] ROUA C. Fused filament additive manufacturing installation comprising an extrusion nozzle and a device for measuring and thermally controlling the method. WO2023017218, n.d.
- [13] Alumentations Documentation 2023. <https://alumentations.ai/docs/> (accessed May 25, 2023).